WETTING BEHAVIORS OF PHENOL- AND UREA-FORMALDEHYDE RESINS AS COMPATIBILIZERS[1]

Sangyeob Lee

Post-Doctoral Research Associate
Department Forest Products and Center for Advanced Vehicular System (CAVS)
Mississippi State University
PO Box 9820
Mississippi State, MS 39762-9820

Todd F. Shupe†

Professor
Louisiana Forest Products Development Center
School of Renewable Natural Resources
Louisiana State University Agricultural Center
227 Renewable Natural Resources Bldg.
Baton Rouge, LA 70803

Leslie H. Groom

Project Leader

and

Chung Y. Hse

Principal Wood Scientist
USDA Forest Service, Southern Research Station
2500 Shreveport HWY.
Pineville, LA 71360

(Received July 2006)

ABSTRACT

Understanding wetting behavior and surface coverage of resins on a wood surface is important to obtain satisfactory adhesion and optimize adhesive application for wood composite manufacturing. Sessile and micro-droplets of urea- and phenol-formaldehyde (UF and PF) resins were generated on wood surfaces to observe wetting behaviors using three directional image generation system and atomic force microscopy (AFM). The generated micro-droplet sizes varied in diameter from 1–100 μm and showed differing wetting behavior based on droplet size and surface conditions. Rougher wood surfaces prevented micro-droplet spreading and resulted in higher contact angles. Contact angles along the fiber direction of the earlywood significantly differed from the angles collected across the fiber direction. Sessile droplet models and dimensionless droplet shape factors (DSF) were used to develop the parameters governing the droplet shape changes from a spherical droplet to an enclosing hemispherical droplet for early- and latewood surfaces. Droplet dispersing areas with earlywood showed 111% with UF and 42% for PF faster changes along the fiber surface as compared to across the fiber surface.

Keywords: Wetting, sessile, micro-droplet, thermosets, droplet shape factors (DSF), atomic force microscopy (AFM).

---

† Member of SWST.

[1] This paper (No. 06-40-0293) is published with the approval of the Director of the Louisiana Agricultural Experiment Station.

INTRODUCTION

Previous wetting studies involving contact-angle measurement on wood surface wettability have shown an old and well-defined technique with model liquid called probes (Gardner et al. 1991; Wålinder 2000; Wålinder and Ström 2001). Wetting studies with wood fiber plastic composites (WPC) have evaluated qualitative surface chemistry and treatment effects on the surface determined by contact-angle analysis to reveal chemical bonding evidence between fibers (Felix and Gatenholm 1991; Hedenberg and Gatenholm 1995; Geoghegan and Krausch 2003). Untreated wood materials were highly hydrophilic, but this was substantially reduced by chemical and physical surface modification (Matuana et al. 1998a; Gauthier et al. 1999; Rabinovich 2002). Improved contact-angle measurements of the modified surfaces were positively correlated to shear strength properties at the interface. Single lap-shear-joint tests and peel tests (Kolosick et al. 1993; Chen et al. 1995; Matuana et al. 1998b; Oksman and Lindberg 1998) were used to investigate surface interactions at the wood-polymer interface. Assuming that the failure of samples occurred at the interface and that the stress distribution was uniform, peel and lap shear strengths can be considered as a qualitative measure of interfacial adhesion. In practice, contact-angle measurements can be readily obtained on flat wood surfaces but not on fibers. However, wetting studies using thermosets such as urea-formaldehyde (UF) and phenol-formaldehyde (PF) resins have rarely been reported due to the incompatibility of thermosets in contact with a thermoplastic matrix.

Some factors influencing surface wetting of wood by liquid monomers and polymers were evaluated to study their effect on flexural and shear strength properties of wood-based products as well as surface energetic properties at the interface (Hse 1972a, 1972c; Shupe et al. 1998). The previous research was based on contact angle at the liquid-solid interface. Limited studies have been made to study wetting of solid wood by contact-angle measurement of sessile or micro-droplets of thermoset resins where the effect of wood structure was considered. The dispersing area of thermoset droplets was influenced by wood structure, grain directions, glueline thickness, viscosity, molecular weight distribution, surface roughness, and surface chemistry (Hse 1968, 1971, 1972a, 1972b; Gardner et al. 1996; Liu et al. 1998; Hse and Kuo 1988; Richter et al. 1994). Mathematical expressions on the droplet volume were based on the response of equivalent height and average contact angle of droplets with an assumption of the symmetric droplet dispersing on the wood surface (Chatterjee 2002a, 2002b). However, surface roughness at the local sites is heterogeneous due to the cellular structure of wood and different grain angles of the wood specimens.

Cazabat (1992) has shown that the wetting behaviors between macro- and micro-droplets on the wood surface were different. To determine the optimum level of thermoset and thermoset wetting characteristics for the wood-based composites, more wetting studies were performed (Casilla et al. 1981; Chibowski and Perea-Carpio 2002; Sharma and Rao 2002; Paunov 2003). Therefore, this study examined the differences between the behavior of micro-sized adhesive droplets on the earlywood and latewood of loblolly pine (*Pinus taeda* L.). This study also addressed droplet behavior such as contact angle of thermosets on the surface of microtome sections, heterogeneous wetting, and interfacial strength properties between thermosets applied wood surface and isotactic polypropylene (iPP) film. The droplet versus scanning method for the contact-angle measurement on a wood surface was also examined.

MATERIALS AND EXPERIMENTAL

Materials

Earlywood and latewood from the sapwood of loblolly pine were selected from areas around Pineville, LA. Wood samples were microtomed with each tangential section of $1.4 \times 1.4 \times 0.06$ cm^3. The wet microtomed samples were placed between glass plates and dried for 48 hours at

80°C. To minimize sample warping, a slight load was applied. Isotactic polypropylene (iPP) films (Plastic Suppliers, Inc. Columbus, OH) were used to make lap-shear joints. Two liquid thermosets—urea-formaldehyde (UF; Dynea Inc., Chembond® YTT-063-02, 60% solids content) and phenol-formaldehyde (PF: Dynea 13B410, 0.1 Pa·S, Sp. Gr.: 1.202 $g \cdot cm^{-3}$, 56% solids content) resin were used as probe droplets.

Three directional images

Three image-capture systems (SPOT RT camera, and two of SOAR VL-7EX; Scalar, Inc., Los Gatos, CA) and an image-analysis system (Image-Pro® Plus, V.5.2) were used to generate continual micro-images from sides (along and across the grain direction) and top for 5 minutes. Figure 1 shows the experimental setup to measure wetting characteristics of UF and PF from the sides and top as a function of time. Contact-angle measurement used a sessile droplet method with microscopic magnification at 50×. Two video capture systems were set up from the top and the side of the sample droplet. An auto-pipette generated 2-μl micro-droplets to observe droplet behavior on the different wood surfaces. Single images were generated from the video files every 5 seconds for 5 minutes. During this stage, droplet size and volume changes were also recorded as a function of time.

Atomic force microscope (AFM) scanning

The technical feasibility of using AFM as a micro-manipulator to measure micro-contact angle measurement and its difference with sessile droplets using resins as a probe material was determined. Figure 2 shows the 3-D plot of the surface and section analysis of the scanned surface. The measurement of the topography of a sample using AFM involves a micro-fabricated cantilever with a very small tip being scanned above the surface of the sample (Wang et al. 2001). The scanning method used a Nanoscope IIIa atomic force microscope (AFM; Digital In-

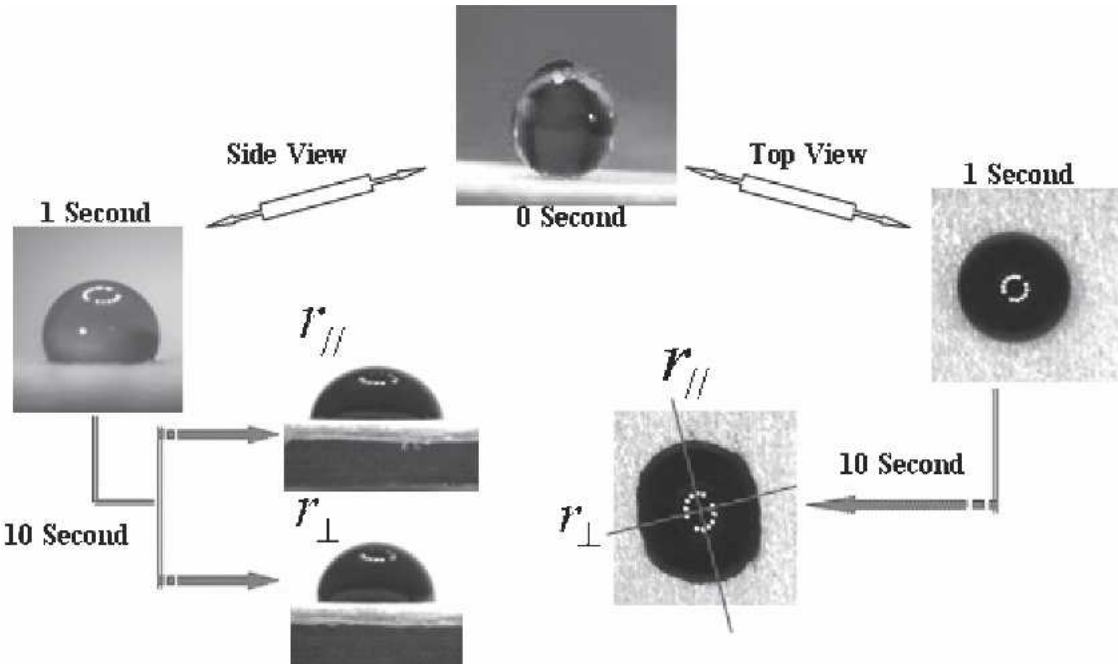

FIG. 1. Experimental procedures to collect phenol-formaldehyde resin wetting characteristics from the sides and top of the instrumental setup as a function of time.

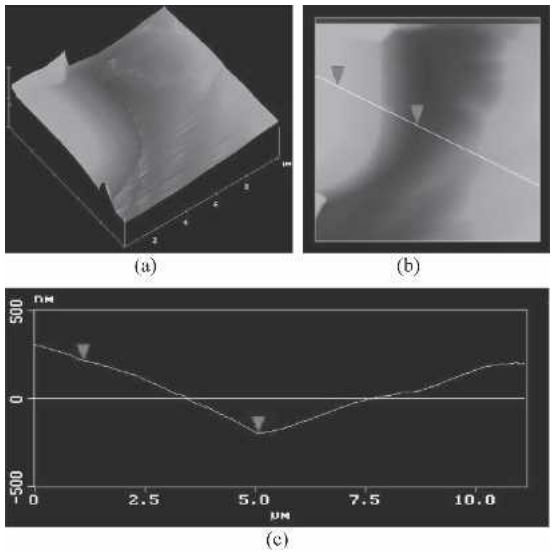

FIG. 2. Atomic force microscopy (AFM) 3D images scanned at the edge of a micro-droplet and section analysis: (a) 3-D surface plot, (b) Section selection, and (c) Section analysis.

struments) mounted on a pneumatic isolation table with an acoustic hood over the dried droplet surface. All AFM micrographs were taken at a resolution of 512 × 512 pixels in tapping mode™. Micro-droplets were generated using an air-automated spray, and the size range was from 1 to 100 μm. The micro-droplets were dried for 24 hours before scanning the wood surface. For the contact-angle measurements, two image-analysis systems were applied. The analysis systems were section analysis from the AFM software and Image-Pro® Plus.

Wetting characteristics

The geometry of droplets quickly changed into a hemisphere shape in 5 seconds. In another 5 seconds, an exact hemisphere reflected a reduced volume (V) of the droplets (Fig. 3). Thus, experimental and mathematical efforts developed several types of simplified hemispheric models to estimate a precise droplet volume on wood surfaces. The following equation from Zwillinger (2003) described the volume, surface area, and angle of response for a hemisphere and a simplified model for the exact hemisphere:

$$V_a = \frac{1}{3}\pi h^2(3R - h) \tag{1}$$

where R was the hemisphere radius, determined by substituting R for droplet height (h). However, the droplets remained as an enclosing hemisphere shape rather than an exact hemisphere. Thus, the following equation was required to generate an exact volume for an enclosing hemisphere with contact angle (θ) and droplet height (h) determined from the droplets.

$$V_b = \frac{1}{6}\pi h\left(3\frac{h^2}{\tan^2\theta} + h^2\right) \tag{2}$$

Accuracy in the droplet volume was obtained using balance of gravity and capillary forces, and a well-applied "drop volume" method for estimating interfacial tension (Lando and Oakley 1967; Wilkinson and Aronson 1973; Holcomb and Zollweg 1990; Chatterjee 2002a, 2002b). A

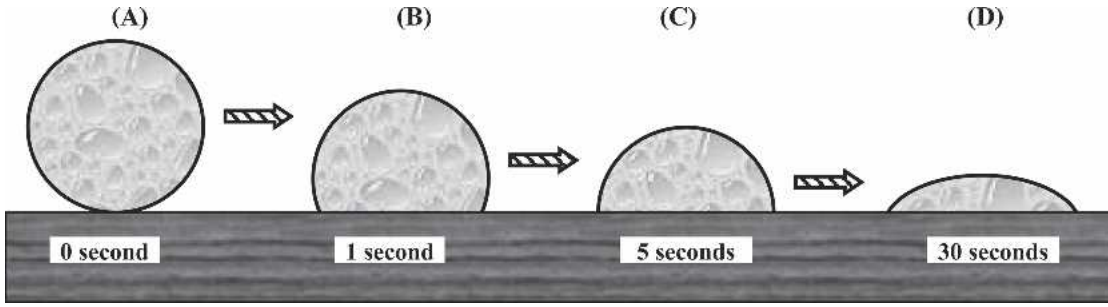

FIG. 3. An enclosing hemispherical dimension of the micro-droplets from an exact circle of an adhesive droplet as a function of time on the wood surface. (A) Exact sphere, (B) Hemisphere, (C) Exact hemisphere, and (D) Enclosing hemisphere.

drop of resin on the wood surface changed with gravity forces, and a relatively small amount of droplets penetrated into the wood surface. The surface tension equation was extracted by using capillary force response for droplet retention on the solid surface and each volume condition. The extracted critical surface tension equations (Eqs. 3 and 4) were expressed as:

$$\gamma_{V_a} = \frac{\Delta\rho g R(2 - 3\mathrm{Cos}\theta + \mathrm{Cos}^2\theta)}{6\mathrm{Sin}\theta} \qquad (3)$$

and

$$\gamma_{V_b} = \frac{\Delta\rho g H}{12 r \mathrm{Sin}\theta} \qquad \left(H = \left[3\frac{h^2}{\tan^2\theta} + h^2\right]\right) \qquad (4)$$

where

$\Delta\rho$ = density difference between the drop and continuous phase
g = gravity acceleration
γ = interfacial tension between the two phases
r = wetted radius
θ = three-phase contact angle
H = total height

Shape analysis

A dimensionless shape factor (DSF: Eqs. 5 and 6) was also generated from the capillary forces ($C_p = [(\Delta\rho g V_{a,b}) - (2\pi\sigma \cdot r\mathrm{Sin}\theta)/A]$) and wet area (A) of the resin droplets (Kwok et al. 1997; Chatterjee 2002a, 2002b). The DSF from each volume condition was calculated and expressed as:

$$DSF_{Va} = \frac{\Delta\rho g R^2}{2\sigma} = \frac{3\mathrm{Sin}^2\theta}{2 - 3\mathrm{Cos}\theta + \mathrm{Cos}^2\theta} \qquad (5)$$

and

$$DSF_{Vb} = \frac{\Delta\rho g R^2}{2\sigma} = \frac{6\mathrm{Sin}^2\theta}{2 - 3\mathrm{Cos}\theta + \mathrm{Cos}^2\theta} \qquad (6)$$

Single lap-shear test

Shear strength properties of the single-lap laminates were tested in tension using an Instron 4465 mechanical testing at a crosshead speed of 0.13 cm·min.$^{-1}$ according to ASTM D5573-94 (ASTM 1994). Figure 4 shows a schematic draw for the shear test. The figure also shows interfaces between resin-applied wood surface and thermoplastic films. Seventy-two PP film laminated joints were prepared with a nominal UF and PF sprayed area of 1.1 × 1.0 cm^2. On each side of the wood strips, a UF or a PF resin was sprayed, and six sheets of PP film were placed in the middle of the strips to address the interfacial shear development at the resin and polymer interface. The single lap-shear specimens were pressed at 0.69 MPa for two minutes at 204°C. At least 18 specimens were tested for each set of samples. Analysis of variance was used to determine the potential significance of the main effects for this study with each resin and wood type. Multiple comparisons were employed to determine significant differences between the different species using SAS software 9.0e (SAS 2004).

Fracture surface

Shear failure was observed using scanning electron microscopy (SEM; S-3600N) on the fracture surfaces of UF- and PF-loaded microtomed wood surfaces and PP film joints, and the investigated interfacial adhesion characteristics at the resin sprayed wood surface and the PP interface. An ion sputter apparatus (Technics Hummer V) was used to coat samples with an approximately 15-nm thin gold layer. Images of 75× and 4,000× were generated at 10 kV.

RESULTS AND DISCUSSION

Shape transformation

Figure 3 shows droplets shape changes from an exact sphere of an adhesive droplet to an enclosing hemispherical dimension as a function of time on the wood surface. The droplet shapes were transformed from an exact sphere with an initial contact angle of 162° to a hemisphere over time (showing little wetting). The shape transformation occurred quickly, in 5 seconds,

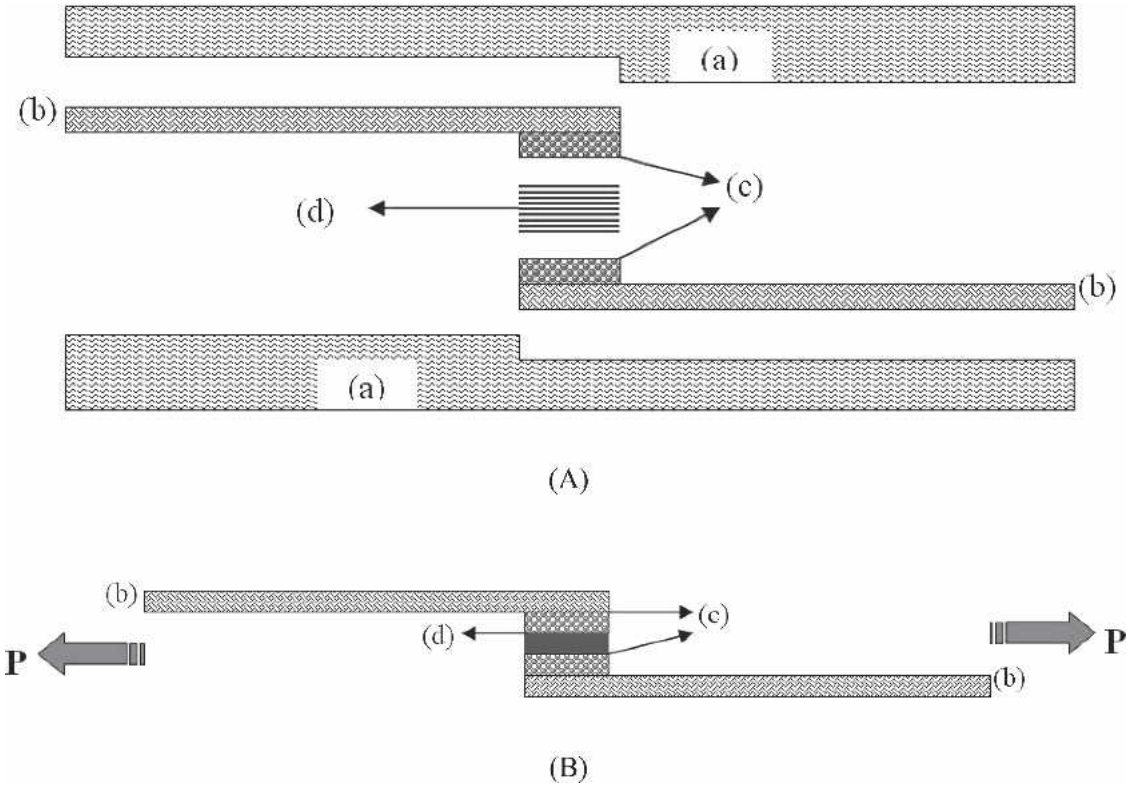

FIG. 4. Sample schemes for single lap shear test. (A) = Shear sample fabrication, (B) = Shear test, (a) = plates, (b) = wood strips, (c) = Resin, and (d) = Polypropylene film.

from an exact sphere to an exact hemisphere shape. From this result, the critical surface tension and volume were calculated using Eqs. (1), (2), (3), and (4). The surface free energy and droplet volume were obtained by using the response of equivalent height of droplet changes (Eq. 1) and the response of the average angle (Eq. 2). Where the droplets were extended by the gravity factor and surface condition of the wood surface, both methods were judged to be reliable to address substrate characteristics interfaced with the two resins. Using the two methods, an increased precision to predict volume changes was obtained. Additionally, droplet dispersing areas covered by resin types were also differentiated on the wood types and fiber directions. Resin droplets dispersed much faster along the fiber direction than across the fiber direction with earlywood and resulted in increased droplet dispersing areas. The areas with earlywood showed 111% (UF) and 42% (PF) faster changes along the fiber surface as compared to across the fiber surface (Top view after 10 seconds in Fig. 1).

Urea-formaldehyde and phenol-formaldehyde wetting

Wetting characteristics of UF and PF droplets on the microtomed wood surface of loblolly pine earlywood and latewood are presented in Table 1. Earlywood with UF droplets dispersed relatively quickly in the longitudinal direction on the surface with higher capillary pressure and the long fiber length. Weight changes were also higher than other combinations. The cell cavities of earlywood are much larger than those of latewood, which has both smaller cavities and thicker cell walls (Fig. 8c). Thus, the surface roughness influenced the dispersing factor and

TABLE 1. *Wetting characteristics of micro urea-formaldehyde and phenol-formaldehyde droplets on the microtome section of loblolly pine earlywood and latewood.*

Thermoset type	Wood type	Sp. gr. ($g \cdot cm^{-3}$) (dry)	Capillary pressure ($mN \cdot cm^{-2}$)	Weight change rate ($\mu l \cdot sec^{-1}$)	Dispersing factor $R_{//}/R_{\perp}$	Contact angle @ 10 sec. (°)		Critical tension ($mN \cdot m^{-1}$)	
						$\theta_{//}$	$\theta_{\perp}$	$r_{//}$	$r_{\perp}$
UF	Early	0.55	14.6	0.073	2.11	68.5	70.6	61.3	37.7
	Late		12.1	0.069	1.39	67.5	72.9	48.7	40.6
PF	Early		13.0	0.068	1.42	65.2	78.6	88.7	60.2
	Late		12.2	0.045	1.27	64.1	73.9	53.2	40.2

resulted in more resin penetration into the cell walls. The dispersing ratios ($R_{//}/R_{\perp}$) indicated that adhesives dropped on the earlywood surfaces provided more extended resin coverage than those applied on the latewood surface. In general, the critical surface tension was used to evaluate adhesive bonding characteristics at the interface (Scheikl and Dunky 1998; Wålinder 2000; Khan et al. 2004). Surface tension ($\boldsymbol{r}_{//}$) values were close to published values (Hse 1971) while $\boldsymbol{r}_{\perp}$ was not. There was less penetration into the inner cell structure with latewood regardless of resin type. This result probably influenced the shear performance at the wood-PP interface. Volume changes of UF and PF droplets were shown as a function of time on the wood surface (Fig. 5). After 15 seconds, the droplet volumes were fairly constant. The volume changes with UF droplets on both wood types showed a similar trend as PF except PF on earlywood surfaces. UF resin gels very quickly and has very high molecular weight (MW) distribution, while PF resin has lower MW distribution, respectively.

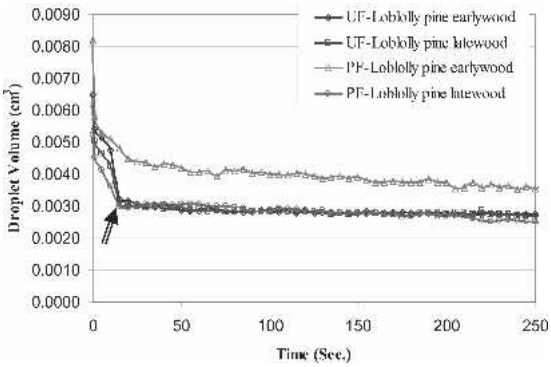

FIG. 5. Volume changes of urea-formaldehyde and phenol-formaldehyde droplets as a function of time on the surface of microtomed loblolly pine wood (Arrow indicates 15 seconds).

Single lap-shear strength

Shear strength properties from single lap joints of the UF and PF sprayed wood surfaces and PP film interface are shown in Fig. 6. Single lap-shear strength increased 53% (from 1.1 MPa to 1.7 MPa) when the latewood was sprayed with UF resin. It should be noted that 88% wood failure was observed with UF resin sprayed on two wood types, while 25% wood failure was noted with PF resin. Single lap-shear tests demonstrated that the UF loading at the wood and PP film interface improved the interfacial interaction. This result is largely attributable to the surface tension of wood with UF droplets due to the inherent properties of this resin. The earlywood, which had higher dispersing ratios with both resin types, showed poor shear performances

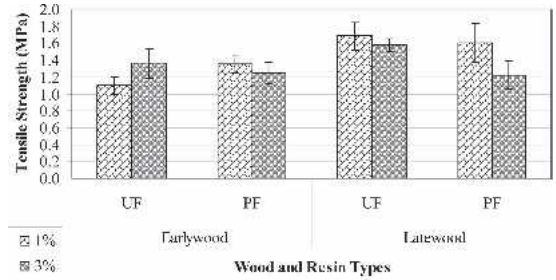

FIG. 6. Shear strength properties from single lap joint laminated assemblies of urea-formaldehyde and phenol-formaldehyde sprayed wood surfaces and polypropylene film interface (The error bars represent one standard deviation).

due to over-penetration by capillary action. Thus, the thermoset resin remaining on the wood surface was beneficial in increasing interfacial interaction at the wood-PP interface with UF resin.

Dimensionless shape factors

Figure 7 shows dimensionless droplet shape factors (DSF) with a critical boundary between high and low retaining regions as a function of contact angle. Loblolly pine had relatively higher retentions with UF resin than PF and influenced shape transformation of the droplets. The higher retention indicates increased resin penetration into the wood and in general, confirms the fact that high resin retention at the interface is important to obtain effective adhesion. Also shear strengths at the wood-PP interface increased and showed a lower thermoplastic failure than when thermoplastics were used for surface modification. Therefore, the capillary forces and surface tension played an important role in influencing the interfacial strength properties.

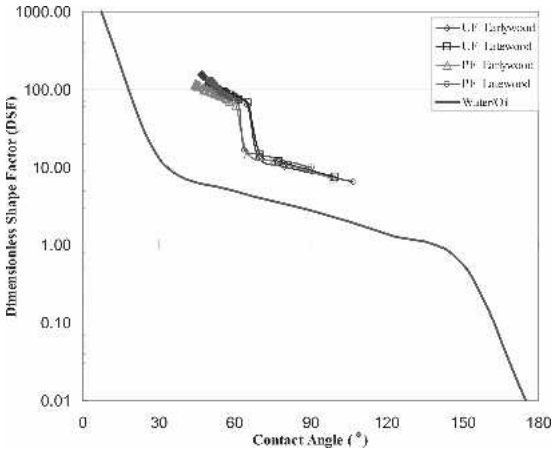

FIG. 7. Dimensionless shape factor (DSF) changes as a function of contact angle changes of urea-formaldehyde and phenol-formaldehyde droplets on earlywood and latewood surfaces.

Contact angle vs. surface scan

Models were developed for contact-angle measurements using two different systems. The models differentiated droplet behaviors on two different wood surfaces. Contact angles from scanned micro-droplets and predicted values with the best-fit models are presented in Table 2. Models were performed with $\alpha = 0.05$. The R^2 values obtained from the models were an excellent fit to the data collected from the micro-droplet scanning method. Micro-droplets sprayed on the wood surfaces showed that wetting on a small scale is strongly affected by minimal physical surface heterogeneities more than the relatively larger scale of sessile droplets and they resulted in higher contact angles. Thus, the AFM technique to scan micro-droplets can be beneficial to understand microscale-droplet behavior of wood adhesives on the surface of wood materials. Experimental contact angles on the wood surfaces were measured using AFM and found to validate prediction models.

Shear failure

SEM micrographs showed the fracture surface from shear load in Fig. 8. The low magnification image shows many fibers exposed from the wood surface. The fibers were produced by PP stretching during the shear failure. PP film sheets were melted under heat and flowed into

TABLE 2. *Model-generated contact angle measurements versus scanned angle of urea-formaldehyde and phenol-formaldehyde droplets on the tangential surface of microtomed loblolly pine.*

Resin	Wood type	Sessile droplet model	R^2	Expected angle (°)	Scanned angle (°)
UF	Earlywood	$Angle = 88.457X^{-0.1215}$	0.88	24.2	28.3
	Latewood	$Angle = 88.334X^{-0.1051}$	0.95	28.8	31.0
PF	Earlywood	$Angle = 90.822X^{-0.0882}$	0.98	35.4	35.5
	Latewood	$Angle = 79.426X^{-0.0835}$	0.94	36.2	39.5

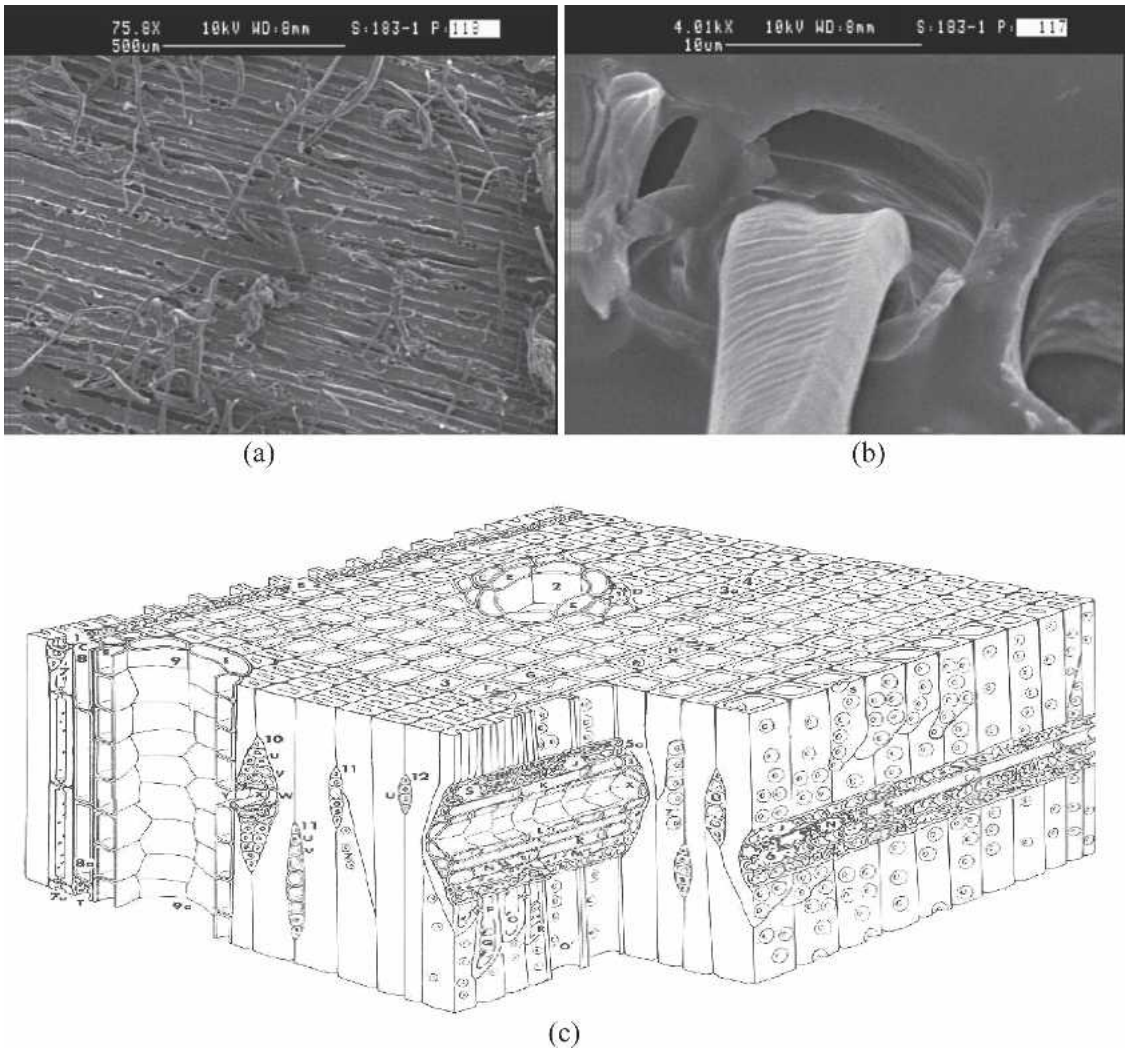

FIG. 8. Scanning electron microscopy (SEM) micrographs generated with (a) low and (b) high magnification on the fracture surface of wood strip and polypropylene interface, and (c) anatomical structures of typical southern pine from Koch (1972).

radial resin canals exposed on the tangential section and the tracheid, parenchyma cells, transverse resin canals, and epithelial cells. The fracture behavior of joints can also be affected by many other variables such as including the fiber and matrix nature, the fiber-matrix interaction, resin distribution, cell structure, etc. Thus, the surface fibrillation of the PP matrix may add the interfacial shear strength of single-lap shear joints.

CONCLUSIONS

Contact angles of resin droplets, heterogeneous wetting, and interfacial strength properties at the interfaces were evaluated on early- and latewood of loblolly pine. The results of a sessile droplet versus scanning method for the contact-angle measurement indicated that micro-droplet behaviors were affected by the cellular structure of the wood surfaces. Two mathematical formulas were developed to represent droplet shape

changes from a sphere to a hemisphere and finally an enclosed hemisphere. The formulas also provided a more accurate means of determining the sessile droplet volume. With regards to the dispersing behaviors of UF and PF resins, the droplets dispersed more easily along the fiber direction. Critical numbers obtained from the force balance equations show a high retention region. Wood structure played an important role in the interfacial shear strength properties.

REFERENCES

American Society For Testing and Materials (ASTM). 1994. Standard practice for classifying failure modes in fiber-reinforced-plastic joints. D 5573-94. American Society for Testing and Materials, West Conshohocken, PA.

Casilla, R. C., S. Chow, and P. R. Steiner. 1981. An immersion technique for studying wood wettability. Wood Sci. Technol. 15:31–43.

Cazabat, A. M. 1992. Wetting from macroscopic to microscopic scale. Adv. Colloid Int. Sci. 42:65–67.

Chatterjee J. 2002a. Shape analysis based critical Eotvos numbers for buoyancy induced partial detachment of oil drops from hydrophilic surfaces. Adv. Colloid Int. Sci. 99:163–179.

———. 2002b. Critical Eotvos numbers for buoyancy-induced oil drop detachment based on shape analysis. Adv. Colloid Int. Sci. 98:265–283.

Chen, M., J. Meister, D. W. Gunnells and D. J. Gardner. 1995. A process for coupling wood to thermoplastic using graft copolymers. Adv. Polym. Tech. 14(2):97–109.

Chibowski, E., and R. Perea-carpio. 2002. Problems of contact angle and solid surface free energy determination. Adv. Colloid Int. Sci. 98:245–264.

Chow, S. 1974. Morphologic accessibility of wood adhesives. J. Appl. Polym. Sci. 18:2785–2796.

Felix, J. M., and P. Gatenholm. 1991. The nature of adhesion in composites of modified cellulose fibers and polypropylene. J. Appl. Polym. Sci. 42:609–620.

Gauthier, R., H. Gauthier, and C. Joly. 1999. Compatibilization between lignocellulosic fibers and a polyolefin matrix. Pages 153–162 *in* R. M. Rowell, ed. Proc. 5th Interl. Conf. Woodfiber-Plastic Composites.

Geoghegan, M., and G. Krausch. 2003. Wetting at polymer surfaces and interfaces. Prog. Polym. Sci. 28:261–302.

Gardner, D. J., N. C. Generalla, D. W. Gunnells, and M. P. Wolcott. 1991. Dynamic wettability of wood. Langmuir 7:2498–2502.

———, M. P. Wolcott, L. Wilson, Y. Huang, and M. Carpenter. 1996. Our understanding of wood surface chemistry in 1995. Pages 29–36 *in* A. W. Christiansen and A. H. Conner, eds. Wood Adhesives. Forest Products Society. Madison, WI.

Hedenberg, P., and P. Gatenholm. 1995. Conversion of plastic/cellulose waste into composites. I. Model of interphase. J. Appl. Polym. Sci. 56:641–651.

Holcomb, C. D., and J. A. Zollweg. 1990. Improve calculation techniques for interfacial tensiometers. J. Colloid Int. Sci. 134:41–50.

Hse, C. Y. 1968. Gluability of southern pine earlywood and latewood. Forest Prod. J. 18(12):32–36.

———. 1971. Properties of phenolic adhesives as related to bond quality in southern pine plywood. Forest Prod. J. 21(1):44–52.

———. 1972a. Surface tension of phenol-formaldehyde wood adhesives. Holzforschung 26:82–85.

———. 1972b. Method for computing a roughness factor for veneer surfaces. Wood Sci. 4(4):230–233.

———. 1972c. Wettability of southern pine veneer by phenol formaldehyde wood adhesives. Forest Prod. J. 22(1): 51–56.

———, and M. L. Kuo. 1988. Influence of extractives on wood gluing and finishing: A review. Forest Prod. J. 38(1):52–56.

Khan, S., Y. H. Chui, M. H. Schneider, and A. O. Barry. 2004. Wettability of treated flakes of selected species with commercial adhesive resins. J. Instit. Wood Sci. 16(5):258–265.

Kolosik, P. C., G. E. Myers, and J. A. Koutsky. 1993. Bonding mechanisms between polypropylene and wood: coupling agent and crystallinity effects. Pages 15–19 *in* M. P. Wolcott, ed. Wood Fiber/Polymer Composites: Fundamental concepts, process, and material options.

Kwok, D. Y., T. Gietzelt, K. Grundke, H. J. Jacobasch, and A. W. Neumann. 1997. Contact angle measurement and contact angle interpretation. 1. Contact angle measurement by axisymmetric drop shape analysis and a goniometer sessile drop technique. Langmuir 13:2880–2894.

Lando, J. L., and H. T. Oakley. 1967. Tabulated correction factors for the drop-weight-volume determination of surface and interfacial tensions. J. Colloid Int. Sci. 25:526–530.

Liu, F. P., T. G. Rials, and J. Simonsen. 1998. Relationship of wood surface energy to surface composition. Langmuir 14:536–541.

Matuana, L. M., R. T. Woodhams, C. B. Park, and J. J. Balatinecz. 1998a. Effect of surface properties on the adhesion between PVC and wood veneer laminates. Polym. Eng. Sci. 38(5):765–773.

———, ———, ———, and ———. 1998b. Influence of interfacial interactions on the properties of PVC/cellulosic fiber composites. Proc. 56th Ann. Tech. Conf. ANTEC. Part 3 (of 3):3313–3318.

Oksman, K., and H. Lindberg. 1998. Influence of thermoplastic elastomers on adhesion in polyethylene-wood flour composites. J. Appl. Polym. Sci. 68(11):1845–1855.

Paunov V. N. 2003. Novel method for determining the three-phase contact angle of colloid particles adsorbed at

air-water and oil-water interfaces. Langmuir 19:7970–7976.

RABINOVICH, Y. I., J. J. ADLER, M. S. ESAYANUR, A. ATA, R. K. SINGH, AND B. M. MOUDGIL. 2002. Capillary forces between surfaces with nanoscale roughness. Adv. Colloid Int. Sci. 96:213–230.

RICHTER, K., W. C. FEIST, AND M. T. KNAEBE. 1994. The effect of surface roughness on the performance of finishes. Research and work reports, EMPA wood dept. Swiss Federal Lab. for Materials Testing and Research, 83 pp.

SAS INSTITUTE INC. 2004. What's New in SAS® 9.0, 9.1, 9.1.2, and 9.1.3. SAS Institute Inc., Cary, NC, USA. 301 pp.

SCHEIKL, M., AND M. DUNKY. 1998. Measurement of dynamic and static contact angles on wood for the determination of its surface tension and the penetration of liquids into the wood surface. Holzforschung 52(1):89–94.

SHARMA, P. K., AND K. H. RAO. 2002. Analysis of different approaches for evaluation of surface energy of microbial cells by contact angle goniometry. Adv. Colloid Int. Sci. 98:341–463.

SHUPE, T. F., C. Y. HSE, E. T. CHOONG, AND L. H. GROOM. 1998. Effect of wood grain and veneer side on loblolly pine veneer wettability. Forest Prod. J. 48(6):95–97.

WÅLINDER, M. 2000. Wetting phenomena on wood: factors influencing measurements of wood wettability. Doctoral Thesis. Dept. Manufacturing System, KTH-Royal Institute of Technology, Stockholm, Sweden. 62 pp.

WÅLINDER, M. E. P., AND G. STRÖM. 2001. Measurement of wood wettability by the Wilhelmy method. Part 2. Determination of apparent contact angles. Holzforschung 55:33–41.

WANG, R., M. TAKEDA, K. MUKAI, AND M. KIDO. 2001. AC non contact mode atomic force microscopy of pure water wetting on natural mica and SUS304 steel. J. Japan Inst. Metals. 65(12):1057–1065.

WILKINSON, M. C., AND M. P. ARONSON. 1973. Applicability of the drop-weight technique to the determination of the surface tension of liquid metals. J. Chem. Soc. Faraday Trans. 69:474–480.

ZWILLINGER D. 2003. CRC: Standard Mathematical Tables and Formulae. 31st edit., Chapman & Hall/CRC Press, Inc., Boca Raton, FL. 910 pp.